

Neural-Augmented Incremental Nonlinear Dynamic Inversion for Quadrotors with Payload Adaptation

Eckart Cobo-Briesewitz, Khaled Wahba, and Wolfgang Hönig

Abstract—The increasing complexity of multirotor applications has led to the need of more accurate flight controllers that can reliably predict all forces acting on the robot. Traditional flight controllers model a large part of the forces but do not take so called residual forces into account. A reason for this is that accurately computing the residual forces can be computationally expensive. Incremental Nonlinear Dynamic Inversion (INDI) is a method that computes the difference between different sensor measurements in order to estimate these residual forces. The main issue with INDI is its reliance on special sensor measurements which can be very noisy. Recent work has also shown that residual forces can be predicted using learning-based methods. In this work, we demonstrate that a learning algorithm can predict a smoother version of INDI outputs without requiring additional sensor measurements. In addition, we introduce a new method that combines learning based predictions with INDI. We also adapt the two approaches to work on quadrotors carrying a slung-type payload. The results show that using a neural network to predict residual forces can outperform INDI while using the combination of neural network and INDI can yield even better results than each method individually.

I. INTRODUCTION

The rise in complexity of tasks to be executed by multirotors has necessitated the development of more accurate flight controllers that are able to model all forces acting on these robots. Traditional flight controllers [1] model a large part of these forces but are unable to model all of them. The remaining forces, called residual forces, can arise from diverse sources such as blade flapping, drag or ground forces [2], [3], [4]. Trying to compute residual forces directly can be computationally complex and intractable for real time control, especially on quadrotors with restricted hardware.

Recent work has shown that learning algorithms can lead to significant improvements in flight performance [4], even modeling the interaction forces between multiple quadrotors [2]. By only learning the residual forces rather than the full dynamics of the quadrotor, the amount of training data needed is greatly reduced. In addition, learning models can help to improve flight performance when sensor readings are noisy or lacking.

Incremental Nonlinear Dynamic Inversion (INDI) [5] is an approach that calculates the residual forces by inverting the standard dynamics model of the system and adjusting the control outputs accordingly. Most implementations rely on special sensor measurements such as rotor RPM on a

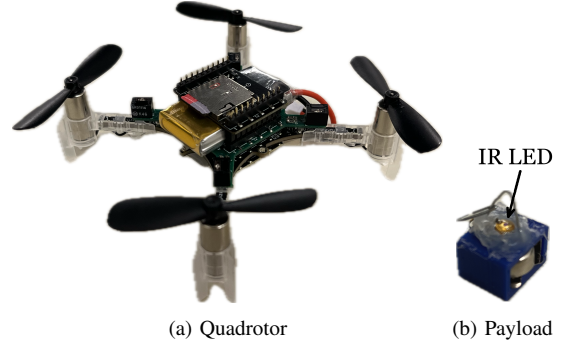


Fig. 1. Hardware used for flight experiments. We rely on a Bitcraze 2.1 with standard motors, uSD-card extension, and custom RPM measurement board that uses IR-LEDs. These LEDs can also be tracked by a motion capture system. The payload is equipped with another active IR LED for tracking.

quadrotor. While INDI can greatly improve flight performance in Unmanned Aerial Vehicles (UAVs), it relies on special sensor measurements that might not be available, and can still produce noisy predictions.

One promising application of multirotors is payload transportation, particularly in time-sensitive fields such as medicine and rescue operations. Some literature also looks into flight controllers for robots carrying a payload attached by a cable [6] [7]. In this setup, the dynamics of the multirotor become more complex due to the inclusion of the payload, which introduces additional forces on the system. These added dynamics can give rise to new types of unmodeled residual forces, thereby increasing the need for accurate estimators and making residual force prediction even more crucial.

We propose to improve the INDI controller by replacing its prediction model with a neural network and applying it to a traditional flight controller [1], removing the need for special sensor measurements and allowing for less noisy residual force computation. We also propose an approach that combines both the predictions of a neural network and INDI to combine the benefits of both approaches. In addition, we apply the same methods to a quadrotor carrying a payload.

II. RELATED WORK

Several prior works have pointed out that INDI is crucial for achieving good tracking performance, especially for high-speed flights. In particular, adding the INDI component is necessary for both MPC and geometric controllers and both kinds of controllers can reach similar flight performance, given a valid reference trajectory [8]. Including a drag

Technical University of Berlin, Berlin, Germany
cobo-briesewitz@campus.tu-berlin.de.

We thank Pia Hanfeld for help with the learning procedure.

The research was funded by the Deutsche Forschungsgemeinschaft (DFG, German Research Foundation) - 448549715.

model [8, 9] or motor delay [10] can further improve the performance, but with a less significant impact. Recently, INDI has also been shown to be important for agile flights with multirotors carrying payloads [11].

Another option is to learn a function that predicts the non-linear residual dynamics, rather than estimating them online as in INDI. The paper by Bauersfeld *et al.* [4] proposes the addition of a neural network to predict residual forces acting on a quadrotor. It makes a non-markovian assumption, which means the network takes previous states as input rather than just the current state. The network predicts a six dimensional vector which contains the residual forces and torques in the x -, y - and z -axis. The results show a clear sign that such additions to a flight controller can improve overall flight performance. Another paper by Shi *et al.* [12] looks into the residual forces coming from the interaction between multiple quadrotors and the downwash effect, which arises when a quadrotor flies over another creating forces pushing the lower one down. In their work they use deepsets to combine the outputs of individual neural networks for each quadrotor to predict the residual forces acting specifically on the z -axis. The method described in this paper reduced the worst-case z -error of a quadrotor's position by a factor of two to four for quadrotors experiencing downwash.

Recent studies [13, 14] have explored integrating the INDI formulation with learning-based models. The approach in Ignatyev *et al.* [13] employs Gaussian Processes to correct sensor measurement inaccuracies in real-time, contrasting with our method as it updates the Gaussian process online but does not fully replace INDI. In contrast, Zhang *et al.* [14] applies meta-learning to continuously refine residual predictions while using INDI, which differs from our approach in that it updates a neural network during flight to predict the control effectiveness matrix of INDI. In our method, however, the model is trained only once and then used to predict the INDI outputs directly.

There exists also some literature that combines learning methods with slung type payload transport with multirotors. The paper by Jin *et al.* [15] uses a neural network to directly predict the forces acting on a multirotor caused by an unknown payload. In our work we assume to know the payload and purely concentrate on residual dynamics.

The main difference of our approach compared to previous work is that it can remove the need for special sensor measurements while also smoothing the residual predictions originally made from these.

III. PROBLEM DESCRIPTION

We first introduce the dynamics that we consider in this work, followed by the control problems that we try to solve.

A. Multirotor Dynamics

Consider a multirotor modeled as a rigid floating base with state $\mathbf{x} = (\mathbf{p}, \mathbf{R}, \mathbf{v}, \boldsymbol{\omega})^\top$. Here, $\mathbf{p}, \mathbf{v} \in \mathbb{R}^3$ represent the position and velocity in the world frame, $\mathbf{R} \in SO(3)$ represents the rotation matrix from body to world, and $\boldsymbol{\omega} \in \mathbb{R}^3$ is the angular velocity expressed in the body frame.

The action $\mathbf{u} \in \mathbb{R}^4$ is defined as the angular velocities of the rotors, $\mathbf{u} = (\omega_1, \omega_2, \omega_3, \omega_4)^\top$. The dynamics are derived from Newton-Euler equations for rigid bodies as

$$\dot{\mathbf{p}} = \mathbf{v}, \quad m\dot{\mathbf{v}} = f_u \mathbf{R} \mathbf{e}_z - mg \mathbf{e}_z + \mathbf{f}_a, \quad (1)$$

$$\dot{\mathbf{R}} = \mathbf{R} \hat{\boldsymbol{\omega}}, \quad \mathbf{J} \dot{\boldsymbol{\omega}} = \mathbf{J} \boldsymbol{\omega} \times \boldsymbol{\omega} + \boldsymbol{\tau}_u + \boldsymbol{\tau}_a, \quad (2)$$

where m is the mass, \mathbf{J} is the inertia matrix, g is the gravitational acceleration constant, $\mathbf{e}_z = (0, 0, 1)^\top$, f_u is the total force created by the rotors, $\boldsymbol{\tau}_u$ is the total torque created by the rotors, and $\mathbf{f}_a, \boldsymbol{\tau}_a$ are unknown external forces and torques, respectively.

The relationship between the motor angular velocity and the generated total force and torque on the rigid body is

$$f_i = \kappa_F \omega_i^2, \quad (3a)$$

$$(f_1, f_2, f_3, f_4)^\top = \mathbf{B}_0 (f_u, \boldsymbol{\tau}_u)^\top, \quad (3b)$$

where κ_F is a propeller constant and \mathbf{B}_0 is a fixed and known actuation matrix.

B. Multirotor With Cable-Suspended Payload

Consider a slung type payload attached to the center of gravity of the multirotor. The state now additionally includes the position and velocity $\mathbf{p}_p, \mathbf{v}_p$ of the payload, respectively. The translational dynamics is extended with additional terms [16]:

$$m\dot{\mathbf{v}} = f_u \mathbf{R} \mathbf{e}_z - mg \mathbf{e}_z + T \mathbf{q} + \mathbf{f}_a, \quad (4)$$

$$\dot{\mathbf{p}}_p = \mathbf{v}_p, \quad m_p \dot{\mathbf{v}}_p = -T \mathbf{q} - m_p g \mathbf{e}_z \quad (5)$$

where $\mathbf{q} = \frac{\mathbf{p}_p - \mathbf{p}}{\|\mathbf{p}_p - \mathbf{p}\|}$ indicates the direction of the cable, m_p is the mass of the payload, and T is the cable tension. From (5), the tension can be computed as

$$T = m_p \mathbf{q} \cdot (-\dot{\mathbf{v}}_p - g \mathbf{e}_z). \quad (6)$$

Note that it is not necessary to add a separate \mathbf{f}_a term to the cable dynamics, as such a force indirectly appears in the UAV dynamics through T .

C. Control Problem

Given the nominal models and feasible reference trajectories $\mathbf{x}_r(t)$, we are aiming to find controllers that can minimize the tracking error:

$$\operatorname{argmin}_{\pi} \int_{t=0}^D d(\mathbf{x}_\pi(t), \mathbf{x}_r(t)) dt, \quad (7)$$

where $\pi(\mathbf{x}, \mathbf{x}_r) \mapsto \mathbf{u}$ is the control law that influences the state $\mathbf{x}_\pi(t)$, D the duration of the reference trajectory $\mathbf{x}_r(t)$, and d is a distance metric.

In this work, we augment classical controllers that ignore \mathbf{f}_a and $\boldsymbol{\tau}_a$ with measured and/or predicted components to improve the tracking performance (7).

IV. APPROACH

A. Geometric Control Laws

1) *Multirotor*: An exponentially stable geometric controller for a multirotor computes the desired force and torques as follows [1]:

$$f_u = (-\mathbf{K}_p \mathbf{e}_p - \mathbf{K}_v \mathbf{e}_v + m g \mathbf{e}_z + m \ddot{\mathbf{p}}_d - \mathbf{f}_a) \cdot \mathbf{R} \mathbf{e}_z, \quad (8a)$$

$$\begin{aligned} \boldsymbol{\tau}_u = & -\mathbf{K}_R \mathbf{e}_R - \mathbf{K}_\omega \mathbf{e}_\omega - \mathbf{J} \boldsymbol{\omega} \times \boldsymbol{\omega} \\ & - \mathbf{J} (\dot{\boldsymbol{\omega}} \mathbf{R}^\top \mathbf{R}_d \boldsymbol{\omega}_d - \mathbf{R}^\top \mathbf{R}_d \dot{\boldsymbol{\omega}}_d) - \boldsymbol{\tau}_a, \end{aligned} \quad (8b)$$

where \mathbf{R}_d , $\boldsymbol{\omega}_d$ and $\dot{\boldsymbol{\omega}}_d$ are desired references that can be computed using differential flatness; \mathbf{e}_p , \mathbf{e}_v , \mathbf{e}_R , $\mathbf{e}_\omega \in \mathbb{R}^3$ are errors with respect to this reference (mathematically defined in [1]), and \mathbf{K}_p , \mathbf{K}_v , \mathbf{K}_R , $\mathbf{K}_\omega \in \mathbb{R}^{3 \times 3}$ are diagonal positive gain matrices.

The highlighted parts \mathbf{f}_a , $\boldsymbol{\tau}_a$ are new terms that need to be added to compensate for the disturbance forces.

2) *Multirotor with cable-suspended payload*: The previous control law can be extended to track a cable-suspended load [17]. The controller is a cascaded design, where the first level tracks the position and velocity of the payload, the second level tracks the desired cable direction and its derivative, and the third level tracks the UAVs rotation and angular velocity. The last part is identical to (8b), since the cable is assumed to be attached at the center of gravity and the mismatches between the nominal and the real model is compensated using $\boldsymbol{\tau}_a$.

While it is also possible to compensate for \mathbf{f}_a (on UAV, payload, or both), in our experiments this did not yield to any tracking improvements.

B. Incremental Nonlinear Dynamic Inversion (INDI)

The key idea of the Incremental Nonlinear Dynamic Inversion (INDI) is to estimate \mathbf{f}_a and $\boldsymbol{\tau}_a$ in real-time using IMU and RPM sensor measurements. The INDI controller is implemented on the multirotor dynamics in [5, 10]. The dynamics of the multirotor-payload case differ from the standard case by the force applied by the cable. Therefore, re-arranging (2) and (4) yields

$$\mathbf{f}_a = m \dot{\mathbf{v}} - f_u \mathbf{R} \mathbf{e}_z + m g \mathbf{e}_z - T \mathbf{q}, \quad (9a)$$

$$\boldsymbol{\tau}_a = \mathbf{J} \dot{\boldsymbol{\omega}} - \mathbf{J} \boldsymbol{\omega} \times \boldsymbol{\omega} - \boldsymbol{\tau}_u. \quad (9b)$$

In INDI, f_u and $\boldsymbol{\tau}_u$ are computed from RPM measurements by applying (3), $\dot{\mathbf{v}}$ is measured by the accelerometer, and $\boldsymbol{\omega}$ is measured by the gyroscope. Other values like $\dot{\boldsymbol{\omega}}$ and $\dot{\mathbf{v}}_p$ are estimated numerically, while \mathbf{R} , \mathbf{q} can be computed from the state estimation. For practical purposes, it is important to filter the measured values, e.g., by using a butterworth filter [10]. The online estimated values can be used as additional feedforward terms in any controller, as highlighted in (8).

C. Incremental Learned Nonlinear Dynamic Inversion (IL-NDI)

Using a dataset containing example trajectories with IMU data, RPM data, and state estimates, one can also compute \mathbf{f}_a

and $\boldsymbol{\tau}_a$ using (9). Here, noisy data such as $\dot{\mathbf{v}}$ and $\dot{\boldsymbol{\omega}}$ can be pre-processed with zero-delay filters such as spline fitting. The resulting values of \mathbf{f}_a and $\boldsymbol{\tau}_a$ are the labels of a supervised learning problems.

For the function approximation, we use a multi-layer perceptron (MLP) with 19 inputs, 6 outputs, 3 hidden layers with 24 dimensions each, and Leaky-ReLU activation. The input includes \mathbf{v} , $\dot{\mathbf{v}}$, $\boldsymbol{\omega}$, the first two columns of \mathbf{R} , and the motor PWM signal (which is different from ω_i as it cannot observe motor delays). The output is the residual force and torque $(\mathbf{f}_a, \boldsymbol{\tau}_a)^\top \in \mathbb{R}^6$. The inputs and outputs of the network are scaled using min-max normalization to the range $[-1, 1]$ to mitigate disparities in value magnitudes and enhance training stability.

For pre-processing, we fit splines with cubic polynomial segments minimizing the L_2 error on the datapoints, rather than connecting points exactly. We fit splines on the collected INDI outputs and use this smooth signal as label for the training.

D. Neural-Augmented Incremental Nonlinear Dynamic Inversion (NA-INDI)

Consider that we split the unmodeled dynamics in two parts $\mathbf{f}_a = \mathbf{f}_{a,NN} + \mathbf{f}_{a,INDI}$ and similar for $\boldsymbol{\tau}_a$, where $\mathbf{f}_{a,NN}$ and $\boldsymbol{\tau}_{a,NN}$ are learned functions that were trained using the steps described in Sec. IV-C. Then the INDI control law only needs to reason about the remaining mismatch in the dynamics, namely:

$$\mathbf{f}_a = m \dot{\mathbf{v}} - f_u \mathbf{R} \mathbf{e}_z + m g \mathbf{e}_z - T \mathbf{q} - \mathbf{f}_{a,NN}, \quad (10a)$$

$$\boldsymbol{\tau}_a = \mathbf{J} \dot{\boldsymbol{\omega}} - \mathbf{J} \boldsymbol{\omega} \times \boldsymbol{\omega} - \boldsymbol{\tau}_u - \boldsymbol{\tau}_{a,NN}. \quad (10b)$$

V. EXPERIMENTS

In order to quantify the performance of the different approaches, we perform real world flights on a set of different trajectories.

A. Physical Setup

We use the Bitcraze Crazyflie 2.1 quadrotors for our experiments, a small quadrotor with an arm length of 4.6cm and weight of 34.7g. It is operated by an STM32 microprocessor (168 MHz, 1 MB of flash, and 192 KB RAM). We equip the standard robot with two additions: a commercially available PCB to log data on a microSD card¹, and a custom PCB to measure RPM as can be seen in Fig. 1 a). In order to accurately predict the position of the quadrotor, we use an OptiTrack motion capture system running at 100 Hz in a $7.5 \times 4 \times 2.75 m^3$ flight space. The custom PCB to measure RPMs uses infrared emitter/receivers and can be used as an active marker by the Optitrack motion capture system to estimate the robot's pose. Rotors have reflective markers underneath the blade, which allow the IR receiver to count the rotor rotations. For communicating with the quadrotor we use Crazyswarm2 which is based on Crazyswarm [18] but uses ROS 2 [19].

¹<https://www.bitcraze.io/products/micro-sd-card-deck/>

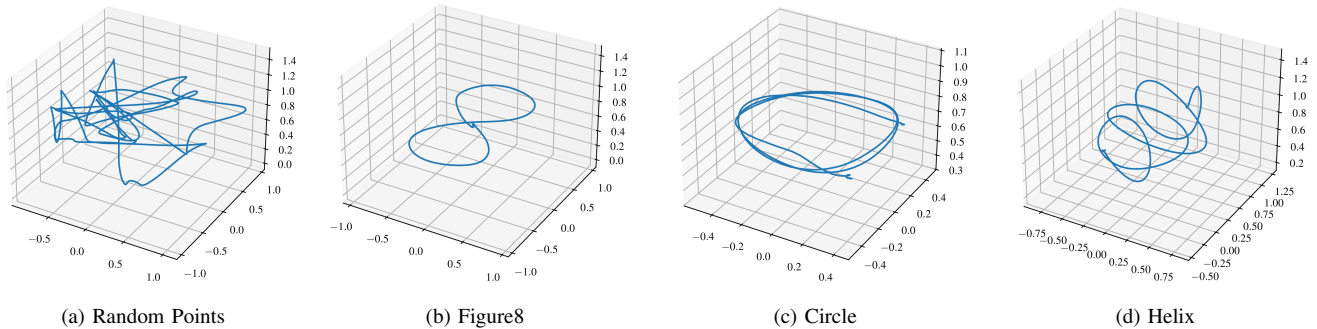


Fig. 2. The first image (a) shows a sample trajectory of those used to generate training data for the neural network, where random points get sampled from a predefined bounding box, to which the quadrotor flies at a random speed from 1 to 8 m/s. The last three images (b), (c) and (d) show the trajectories used for testing the performance of the different controllers.

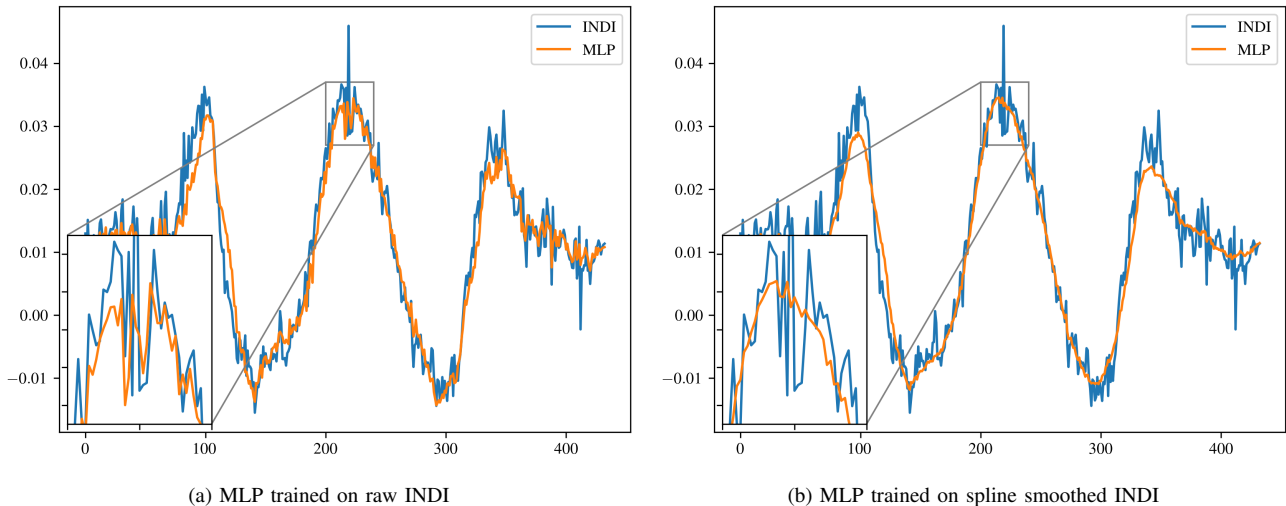


Fig. 3. The figure shows the outputs of two different MLPs on the residual forces in the x-axis and the original INDI predictions on a Figure8 flight path. Predictions of the MLP when trained on (a) the raw INDI outputs and (b) INDI outputs with spline fitting pre-processing. While the standard MLP has some de-noising properties, it outputs smoother predictions when trained on less noisy data.

For the payload scenario we use a $5g$ weight attached at the center of the quadrotor by a string with $0.5m$ length. The string is connected to the quadrotor by a magnet. The payload is also equipped with an infrared LED for estimating its position as can be seen in Figure 1 b). We estimate the velocity and the acceleration of the payload using filters.

B. Data Collection and Training

We train our neural networks on a set of trajectories generated by sampling random positions inside of a predefined bounding box with dimensions $1.6 \times 1.6 \times 0.4m^3$, to which the quadrotor travels at a randomly sampled velocity of up to 8 m/s for the no payload case and 5 m/s for the payload case.

We collected a total of 164,661 timestamps, or around 30 minutes of flight data, for the no-payload scenario each one being a pair of state and residual force and torque, and 78,493 timestamps or around 15 minutes for the payload scenario. These random flights cover a wide range of quadrotor states.

We use the the ADAM optimizer [20] with an L1-loss and with an initial learning rate of $3e-4$ while reducing the

learning rate by a factor of 0.92 every 10 epochs to enhance training stability and convergence, training for a total of 128 epochs. We train two separate neural networks, one for the payload case and one without a payload with the same neural network architecture and training process, while only changing the training data.

We run all neural networks locally on the quadrotor hardware. For the MLP described in Sec. IV-C, the inference time is 202.86 microseconds, corresponding to a frequency of 4930 Hz, when running on the Crazyflie hardware.

C. Testing Scenarios

We then test the performance of the controllers on three different predefined trajectories which are not present in the training set. The trajectories can be seen in Figure 2. We average the performance of each controller over 10 flights for each trajectory. For our error metric we use the average euclidean distance between the quadrotor (or the payload) and the desired trajectory over all timestamps. We do the same experiments for both the payload and no payload scenarios, with the only difference being the speed. For the

TABLE I

COMPARISON OF AVERAGE DEVIATION FROM DESIRED FLIGHT PATH (METERS) OF THE QUADROTOR WITH NO PAYLOAD.

	Circle	Figure8	Helix
Lee	0.0752 ± 0.0122	0.0729 ± 0.0031	–
INDI-cf	0.4746 ± 0.0053	0.4743 ± 0.0215	0.3172 ± 0.0041
INDI-PWM	0.1827 ± 0.0097	0.1889 ± 0.0182	–
INDI	0.0455 ± 0.0024	0.0453 ± 0.0031	0.0316 ± 0.0019
IL-NDI	0.0482 ± 0.0024	0.0432 ± 0.0024	0.0290 ± 0.0015
NA-INDI	0.0450 ± 0.0028	0.0413 ± 0.0013	0.0286 ± 0.0011

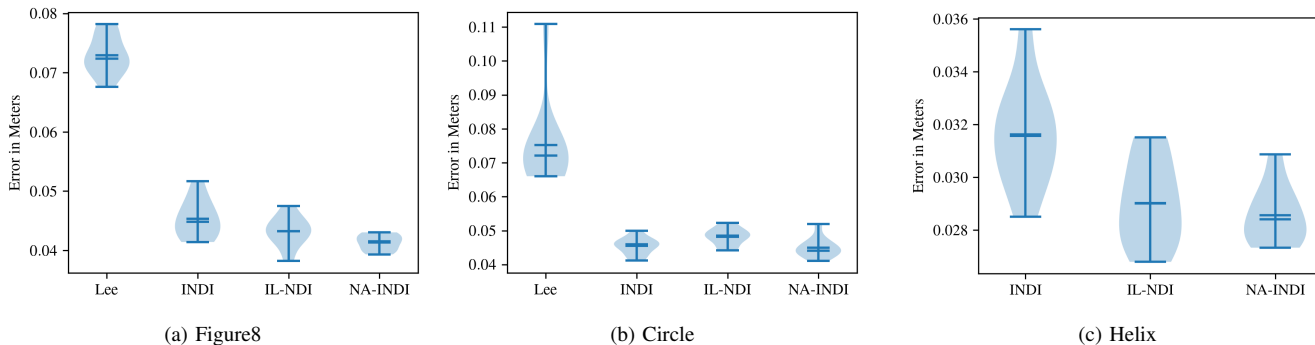


Fig. 4. Error comparison between flights with no payload. For Helix, the standard geometric controller (Lee) was unable to fly.

no payload case the maximum velocity was 1.7 m/s for Figure8, 1.7 m/s for the circle trajectory and 1.6 m/s for helix, while in the payload case the maximum velocities were 1.2 m/s for Figure8, 1 m/s for circle and 1 m/s for helix.

In order to prove the reliance on RPM measurements of INDI, we test the performance of an adjusted version of INDI which uses pulse width modulation values instead of RPM to measure the total force output of the rotors. We also tried testing the default INDI implementation inside of the Crazyflie firmware² but the tracking error was over five times as high as with the Lee controller with no INDI.

D. Results

1) *Multicopter*: Table I and Figure 4 show that the combination of INDI+MLP lead to the highest performance, greatly improving the performance of just the basic geometric controller (Lee). As can be seen from the results, the MLP has a slightly better performance than just INDI. This might be a result of the MLP being trained on a smoothed version of the INDI predictions, which might reduce the noise in the final control signal.

Using the adapted INDI with pulse width modulation measurements (INDI-PWM) leads to the worst performance, highlighting the need for the more precise RPM measurements when using INDI.

For the Helix flight path both Lee and INDI-PWM were unable to fly and would crash each time.

Figure 3 compares the output between two different neural networks, where one is trained on the raw INDI outputs and the second one was trained on data preprocessed by spline fitting. This further highlights the benefits of using a neural network to generate a smooth version of the INDI residuals.

2) *Multicopter with Payload*: In Table II and Figure 5 we can see the results for the experiments done on the multicopter with a payload. The results show that the standard INDI approach performs better compared to IL-NDI or NA-INDI. This might be due to more complex external torques that can be measured in real-time, but are more difficult to predict for the neural network without RPM measurements. Although INDI performs slightly better than IL-NDI, the difference is low for two of the three experiments, showing the potential of using a learning algorithm to remove the need for special sensor measurements in complex systems like this quadrotor carrying a payload.

VI. CONCLUSION

The results of this study demonstrate that INDI can be effectively replaced by a neural network, which, in some cases, achieves superior performance without requiring RPM measurements. While the improvements may be less pronounced when applied to more complex payload systems, the findings highlight the potential advantages of learning-based approaches. These methods not only reduce the reliance on specialized sensors but can also enhance system performance by minimizing output noise.

Future work should investigate adding a residual force rejection in the payload case.

²<https://github.com/bitcraze/crazyflie-firmware>

TABLE II

COMPARISON OF AVERAGE DEVIATION FROM DESIRED FLIGHT PATH (METERS) OF THE QUADROTOR WITH A PAYLOAD.

	Circle	Figure8	Helix
Lee	0.1974 ± 0.0172	0.3014 ± 0.0287	0.1488 ± 0.0332
INDI	0.1263 ± 0.0291	0.1731 ± 0.0223	0.1144 ± 0.0462
IL-NDI	0.1318 ± 0.0233	0.2496 ± 0.0223	0.1197 ± 0.0518
NA-INDI	0.1554 ± 0.0396	0.1829 ± 0.0306	0.1469 ± 0.0557

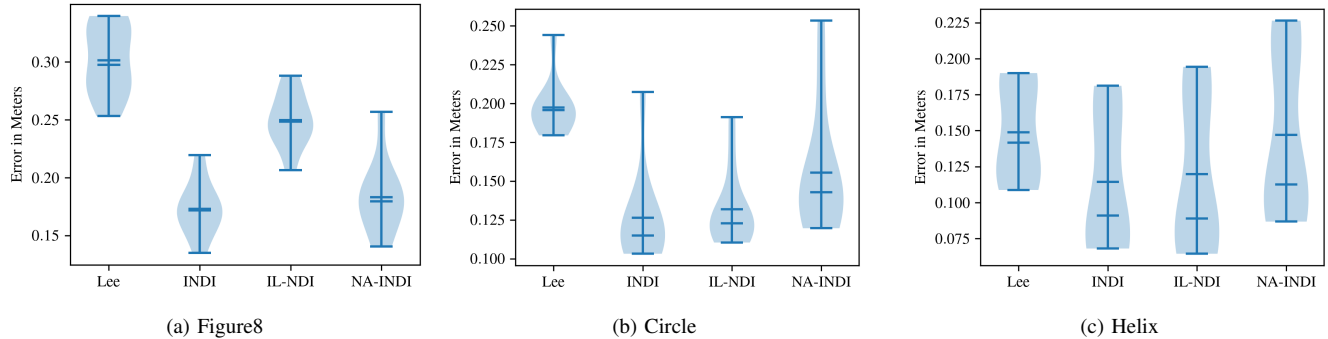


Fig. 5. Error comparison between flights with a payload.

REFERENCES

- [1] T. Lee, M. Leok, and N. H. McClamroch, "Geometric tracking control of a quadrotor uav on $se(3)$," in *49th IEEE Conference on Decision and Control (CDC)*, IEEE, 2010.
- [2] G. Shi, W. Hönig, Y. Yue, and S.-J. Chung, "Neural-swarm: Decentralized close-proximity multirotor control using learned interactions," in *IEEE International Conference on Robotics and Automation (ICRA)*, 2020.
- [3] G. Shi, W. Hönig, X. Shi, Y. Yue, and S.-J. Chung, "Neural-swarm2: Planning and control of heterogeneous multirotor swarms using learned interactions," *IEEE Transactions on Robotics*, 2021.
- [4] L. Bauersfeld, E. Kaufmann, P. Foehn, S. Sun, and D. Scaramuzza, "Neurobem: Hybrid aerodynamic quadrotor model," in *Robotics: Science and Systems XVII*, Robotics: Science and Systems Foundation, 2021.
- [5] E. J. J. Smeur, Q. Chu, and G. C. H. E. Croon, "Adaptive incremental nonlinear dynamic inversion for attitude control of micro air vehicles," *Journal of Guidance, Control, and Dynamics*, vol. 39, no. 3, pp. 450–461, 2016, ISSN: 0731-5090.
- [6] S. Tang, "Aggressive maneuvering of a quadrotor with a cable-suspended payload," University of Pennsylvania, Tech. Rep., 2014.
- [7] K. Wahba and W. Hönig, "Efficient optimization-based cable force allocation for geometric control of a multirotor team transporting a payload," in *2023 IEEE International Conference on Robotics and Automation (ICRA)*, 2023, pp. 1234–1240.
- [8] S. Sun, A. Romero, P. Foehn, E. Kaufmann, and D. Scaramuzza, "A comparative study of nonlinear mpc and differential-flatness-based control for quadrotor agile flight," *IEEE Transactions on Robotics (T-RO)*, 2022, Preprint available at https://rpg.ifi.uzh.ch/docs/TRO22_Sun.pdf.
- [9] M. Faessler, A. Franchi, and D. Scaramuzza, "Differential flatness of quadrotor dynamics subject to rotor drag for accurate tracking of high-speed trajectories," *IEEE Robotics and Automation Letters*, vol. 3, no. 2, pp. 620–626, Apr. 2018, ISSN: 2377-3766, 2377-3774, arXiv: 1712.02402 [cs].
- [10] E. Tal and S. Karaman, "Accurate tracking of aggressive quadrotor trajectories using incremental nonlinear dynamic inversion and differential flatness," *IEEE Transactions on Control Systems Technology*, vol. 29, no. 3, pp. 1203–1218, May 2021, ISSN: 1558-0865.
- [11] S. Sun, X. Wang, D. Sanalitra, A. Franchi, M. Tognon, and J. Alonso-Mora, "Agile and cooperative aerial manipulation of a cable-suspended load." arXiv: 2501.18802 [cs]. (Jan. 30, 2025), pre-published.
- [12] G. Shi, W. Hönig, X. Shi, Y. Yue, and S.-J. Chung, "Neural-swarm2: Planning and control of heterogeneous multirotor swarms using learned interactions," *IEEE Transactions on Robotics*, vol. 38, no. 2, pp. 1063–1079, Apr. 2022, ISSN: 1941-0468.
- [13] D. Ignatyev and A. Tsourdos, "Incremental nonlinear dynamic inversion with sparse online gaussian processes adaptation for partially unknown systems," in *2022 30th Mediterranean Conference on Control and Automation (MED)*, 2022, pp. 233–238.
- [14] X. Zhang and M. Ran, "Meta-learning-based incremental nonlinear dynamic inversion control for quadrotors with disturbances," *Applied Sciences*, vol. 13, no. 21, p. 11 844, 2023, Special Issue: Intelligent Unmanned System Technology and Application.
- [15] A. Jin, C. Li, Q. Wang, Y. Liu, P. Huang, and F. Zhang, "Neural predictor for flight control with payload," *arXiv preprint arXiv:2410.15946*, 2024.
- [16] K. Sreenath and V. Kumar, "Dynamics, control and planning for cooperative manipulation of payloads suspended by cables from multiple quadrotor robots," *m*, vol. 1, no. r2, r3, 2013.
- [17] T. Lee, K. Sreenath, and V. Kumar, "Geometric control of cooperating multiple quadrotor uavs with a suspended payload," in *52nd IEEE Conference on Decision and Control*, Dec. 2013, pp. 5510–5515.
- [18] J. A. Preiss, W. Hönig, G. S. Sukhatme, and N. Ayanian, "Crazyswarm: A large nano-quadcopter swarm," in *Proceedings of the IEEE International Conference on Robotics and Automation (ICRA)*, 2017, pp. 3299–3304.
- [19] S. Macenski, T. Foote, B. Gerkey, C. Lalancette, and W. Woodall, "Robot operating system 2: Design, architecture, and uses in the wild," *Science Robotics*, vol. 7, no. 66, 2022.
- [20] D. P. Kingma and J. Ba, "Adam: A method for stochastic optimization," in *Proceedings of the 3rd International Conference on Learning Representations (ICLR)*, 2015.